

## Endurance Brake Classification Control Based on the Generalized Growth and Pruning Radial Basis Function Neural Network

Peilong Shi<sup>a</sup>, Man Yu<sup>a</sup>, Xiongwen Lu<sup>b</sup>, Xuan Zhao<sup>a</sup>

<sup>a</sup>School of Automobile, Chang'an University, China

<sup>b</sup>China FAW Group Corporation R&D Center, China

Corresponding Author, Email: 317273180@qq.com

### ABSTRACT:

Because of the difference of working principles and arrangements of endurance braking systems, including engine brake, exhaust brake and eddy current retarder, it is difficult to match braking manually more than two types of endurance braking systems working simultaneously on long downhill. Meanwhile, manipulating control on different slopes will distract the driver's attention and cause driving fatigue. Aiming at this problem, the endurance brake classification control strategy is proposed, setting the deceleration, road slope and the difference of current speed & target speed as an input and the endurance brake classification as an output variable. Considering velocity variation is related to these factors with strong nonlinear characteristics, Generalized Growth and Pruning Radial Basis Function neural network control is used to estimate the input deceleration. Tests were conducted to verify the accuracy of simulation model. Variable slopes are researched through simulation method. The results show that the system designed to achieve automatic matching control can effectively decelerate and keep the truck running stably.

### KEYWORDS:

GGAP-RBF neural network; Endurance brake; Heavy duty truck; Classification control

### CITATION:

P. Shi, M. Yu, X. Lu, X. Zhao. 2017. Endurance Brake Classification Control Based on the Generalized Growth and Pruning Radial Basis Function Neural Network, *Int. J. Vehicle Structures & Systems*, 9(5), 330-335. doi:10.4273/ijvss.9.5.11.

## 1. Introduction

Using service braking system frequently on long downhill often leads to heat recession. To solve this problem, heavy duty trucks are equipped with endurance braking systems including engine brake, Jacobs brake, exhaust brake, hydraulic retarder and eddy current retarder. The braking power is almost proportional to the engine power. However, increasing braking force by the means of enhancing engine power will lead to rising costs and decreasing fuel efficiency, despite of engine brake relying on the throttle valve, exhaust brake relying on the butterfly valve, eddy current retarder relying on the coil turns and hydraulic retarder determined by liquid filling rate. At the same time, the operating mode varies the principle. Running on downhill, the driver not only manipulates the steering system but also operates the endurance braking systems according to the speed and slopes. In this way, the intensity of the driver's labour is enhanced greatly; the driving safety has dropped obviously. Therefore, the matter to achieve a coordinated control of endurance braking systems is one of the key issues in field of braking safety on the long downhill for heavy duty truck.

Ma [1] researched the retarder brake on flat road and designed a neural network control system utilizing the service brake and retarder brake to reduce the braking distance. Zhao [1] researched the fuzzy control strategy of service brake and retarder on long downhill. Dong [3]

studied the engine brake control through CVT system. Wu [4] analyzed the influence of eddy current retarder to the braking performance of a bus. Yu [5] researched the combined effect of engine brake, exhaust brake and retarder under fixed gear by a designed fuzzy controller. Based on above researches, the endurance brake classification control strategy of a heavy duty truck is proposed, which controls the output endurance braking force according to the demanding braking force during the deceleration stage and relative constant speed stage. In consideration of the nonlinear relationship among deceleration, slope and the difference between current speed and target speed, the Generalized Growth and Pruning Radial Basis Function (GGAP-RBF) neural network is used. The control strategy is verified by simulation and road tests, and achieves preferable effect under variable slopes condition.

## 2. Classification strategy of endurance braking systems

Road tests are conducted to obtain the characteristic models based on vehicle dynamics theory, namely the relationship between braking torque and speed varying with the gears. As to engine brake and exhaust brake, the function relationship is given by,

$$T_{b\_con\_i} = C_i \cdot n^2 + D_i \cdot n + E_i \quad (1)$$

Where  $C_1$ ,  $D_1$ ,  $E_1$  and  $C_2$ ,  $D_2$ ,  $E_2$  are coefficients of engine brake and exhaust brake torque characteristic

model as given in Table 1.  $T_{b\_con\_i}$  is the braking torque. For retarder, the function is given by [1],

$$T_{b\_con\_3} = A_3 \cdot u_a^4 + B_3 \cdot u_a^3 + C_3 \cdot u_a^2 + D_3 \cdot u_a + E_3 \quad (2)$$

Where  $A_3, B_3, C_3, D_3, E_3$  are the coefficients of retarder brake torque characteristic model as given in Table 2.  $u_a$  is the vehicle speed.

**Table 1: Coefficients of engine brake and exhaust brake torque characteristic models**

| Parameter     | $C_i$                  | $D_i$ | $E_i$   |
|---------------|------------------------|-------|---------|
| Engine brake  | $-1.00 \times 10^{-4}$ | 0.45  | -75.04  |
| Exhaust brake | $-1.00 \times 10^{-4}$ | 0.53  | -255.25 |

**Table 2: Coefficients of retarder torque characteristic model**

| Mode  | I                       | II                      | III                     | IV                      |
|-------|-------------------------|-------------------------|-------------------------|-------------------------|
| $A_i$ | $-1.13 \times 10^{-10}$ | $-1.53 \times 10^{-10}$ | $-2.93 \times 10^{-10}$ | $-3.94 \times 10^{-10}$ |
| $B_i$ | $7.02 \times 10^{-7}$   | $9.42 \times 10^{-7}$   | $1.70 \times 10^{-6}$   | $2.27 \times 10^{-3}$   |
| $C_i$ | $-1.59 \times 10^{-3}$  | $-2.14 \times 10^{-3}$  | $-3.67 \times 10^{-3}$  | $-4.89 \times 10^{-3}$  |
| $D_i$ | 1.59                    | 2.17                    | 3.56                    | 4.74                    |
| $E_i$ | -146.97                 | -86.62                  | -249.88                 | -435.81                 |

Distinguishing from the service braking system, endurance braking torque transmit relying on power train system. The braking force acting on the wheel can be given by,

$$F_{b\_con\_ij} = T_{b\_con\_i} i_g i_0 / r \eta_T \quad (3)$$

Where,  $i$  is the form of endurance braking system,  $j$  is the gears or modes.  $F_{b\_con\_ij}$  is the output braking force,  $i_g$  is transmission ratio,  $i_0$  is the final drive ratio,  $\eta_t$  is the mechanical efficiency and  $r$  is wheel rolling radius. As for engine brake and retarder are working simultaneously, the braking force on the wheel can be obtained using,

$$F_{b\_con\_ij} = T_{b\_con\_1j} i_g i_0 / r \eta_T + T_{b\_con\_3j} i_0 / r \eta_T \quad (4)$$

Similarly, the braking force on the wheel can be arrived as exhaust brake and retarder working using,

$$F_{b\_con\_ij} = T_{b\_con\_2j} i_g i_0 / r \eta_T + T_{b\_con\_3j} i_0 / r \eta_T \quad (5)$$

The matching work of 3 endurance braking systems form 14 ways, corresponding to 14 classifications as follows: 1 - exhaust brake; 2 - engine brake; 3 - retarder I; 4 - retarder II; 5 - retarder III; 6 - retarder IV; 7 - exhaust brake + retarder I; 7 - exhaust brake + retarder I; 8 - exhaust brake + retarder II; 9 - exhaust brake + retarder III; 10 - exhaust brake + retarder IV; 11 - engine brake + retarder I; 12 - engine brake + retarder II; 13 - engine brake + retarder III; 14 - engine brake + retarder IV.

The output braking force curves are presented in Figs. 1 to 4 for 5<sup>th</sup>, 6<sup>th</sup>, 7<sup>th</sup> and 8<sup>th</sup> gear respectively. The output endurance braking force increases as shifting to lower gears and for increased speed. The output braking force is smaller while engine brake, exhaust brake or retard I are working alone. Maximum braking force achieved by the way of engine brake and retarder IV working together. For 5<sup>th</sup> gear, the braking force varies from 822N to 24790N, corresponding to a speed of between 11km/h to 31km/h. For 6<sup>th</sup> gear, the braking force range and speed range are 822N to 21997N and 14km/h to 42km/h, respectively. For 7<sup>th</sup> gear, the braking force range and speed range are 822N to 18141N and 20km/h to 58km/h. For 8<sup>th</sup> gear, the braking force range

and speed range are 499N to 17506N and 27km/h to 78km/h, respectively.

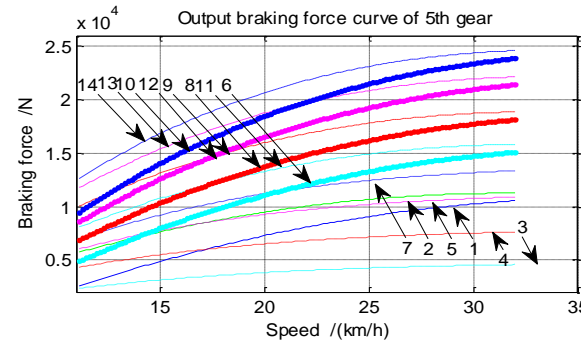


**Fig. 1: Output braking force curve of 5<sup>th</sup> gear**

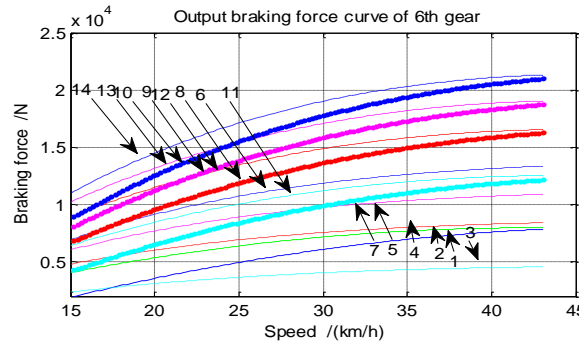


**Fig. 2: Output braking force curve of 6<sup>th</sup> gear**

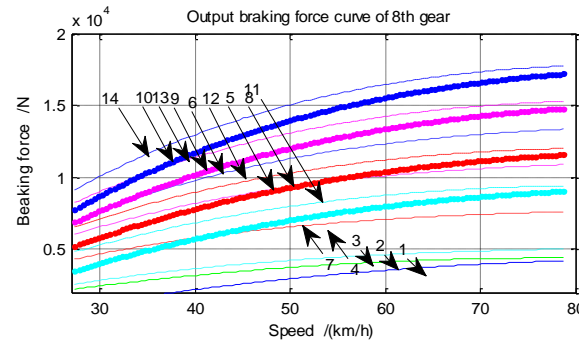


**Fig. 3: Output braking force curve of 7<sup>th</sup> gear**

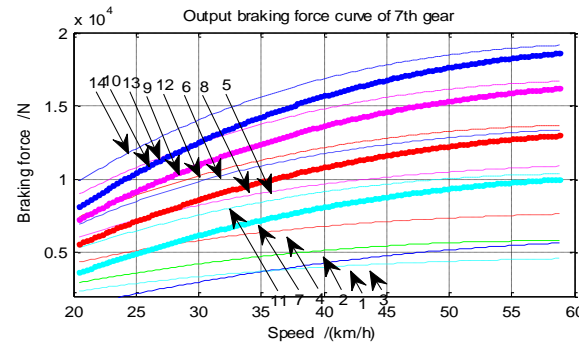


**Fig. 4: Output braking force curve of 8<sup>th</sup> gear**

### 3. Classification control strategy based on GGAP-RBF neural network

#### 3.1. Vehicle dynamics model

Suffering the gravity, the truck has a tendency to accelerate on downhill. Considering safety and stability, it is necessary to provide a brake force. Therefore, the

longitudinal dynamic Eqn. (1) can be derived by force analysis diagram from Fig. 5 as follows,

$$F_t + F_i = F_f + F_w + F_j \quad (6)$$

Where  $F_i$  is gravity component along road,  $F_i = mgi$ .  $F_t$ ,  $F_f$ ,  $F_j$  and  $F_w$  are the driving force, rolling resistance force, acceleration resistance force and air resistance force respectively. The endurance braking working, Eqn. (6) can be rearranged as follows,

$$F_i = F_f + F_w + F_{b\_con} + F_j \quad (7)$$

$$F_{b\_con\_ij} = mgi - (F_f + F_w) - \delta m \frac{du}{dt} \quad (8)$$

Where  $\delta$  is the rotational mass conversion factor and  $m$  is the weight of the test truck.  $F_f + F_w$  was obtained from tests [8],  $F_f + F_w = 0.37u_a^2 + 7.50u_a + 3216.14$ . Eqn. (8) can be further simplified as follows,

$$F(a, u_a, i) = mgi - (F_f(u_a) + F_w(u_a)) - \delta m \frac{du}{dt} \quad (9)$$

The demand of the brake required depends on the slope, driving speed and target deceleration on downhill.

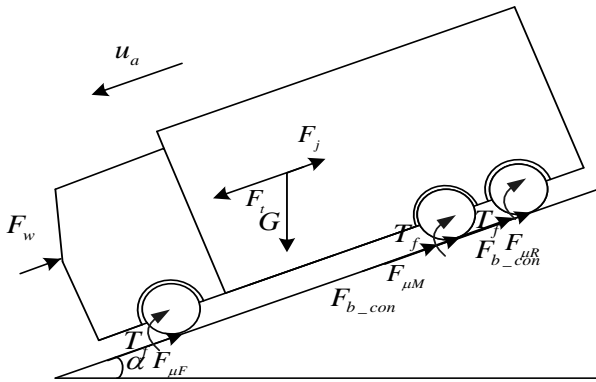


Fig. 5: Force analysis diagram of heavy duty truck on downhill

### 3.2. Classification control strategy of endurance braking systems

In order to adapt to variable slope section, the driver has to manipulate the endurance braking system frequently. At the same time, the driver is handling the steering system and shifts the gear depending on road condition. These processes divert the driver's attention and increase fatigue driving probability. Considering those aspects, this paper proposed a classification control strategy which can realize an intelligent matching control. As shown in Fig. 6, in normal deceleration process, the deceleration is variable, that is, the demand brake force varies with the speed. Although given endurance braking force decreases with the decrease of speed, that is less than demand value. Under these circumstances, we need to manipulate another endurance braking system. As shown in Eqn. (9), factors influencing the demand braking force are slope ( $i$ ), speed ( $u_a$ ) and deceleration ( $a$ ). In order to realize a control strategy, these three factors are selected as input variables and expected speed ( $u_{ae}$ ) as control objective and the difference of expected speed ( $u_{ae}$ ) and current speed ( $u_a$ ) as control variable. The implemented control strategy is shown in Fig. 7. When  $|u_a - u_{ae}| \geq x$  ( $x$  is a threshold), control truck

deceleration, and deceleration depending on  $i$ ,  $u_a$  and  $a$ ; When  $|u_a - u_{ae}| < x$ , judging the truck speed in a stable state, the default deceleration is 0. In the two states, the endurance braking level is determined by  $|F(a, u_a, i) - F_{b\_con\_ij}(u_a)|_{min}$ .

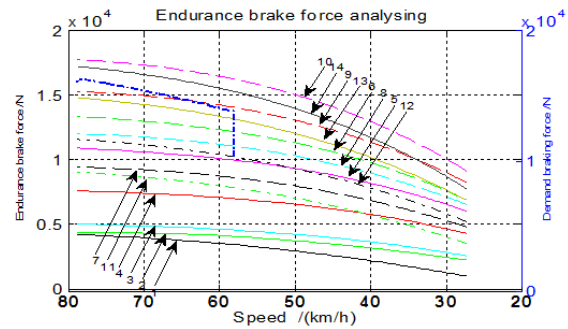


Fig. 6: The demand braking force at different classifications

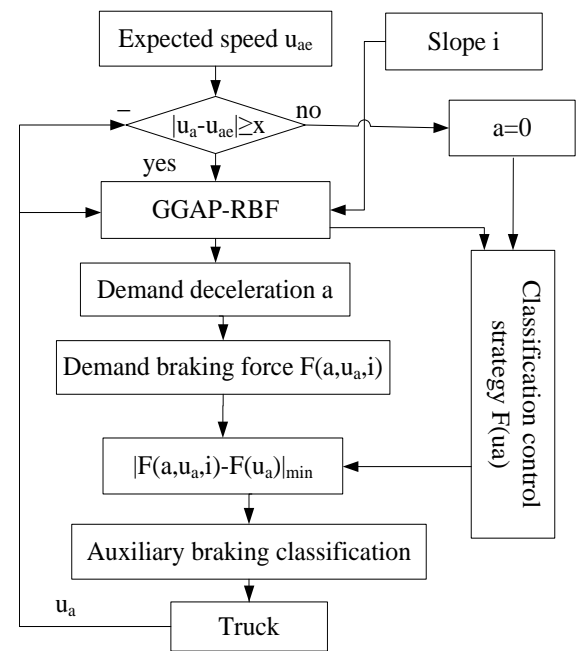


Fig. 7: Flow chart of the control strategy

### 3.3. Deceleration estimation based on GGAP-RBF neural network

The output deceleration is determined by road condition, truck state, speed, target speed, etc. It is really hard to establish exact mathematical model considering these factors given their strong nonlinear relationship. Focusing on these issues, this paper adopts the neural network model to predict the deceleration. The advantage of the neural network is no need to establish an accurate model of input-output relations, perform well in strong nonlinear mapping ability, self-learning ability and good adaptability. However, the traditional back propagation neural network is easy to fall into local optimum, and network training takes too much time. For improving the global approximation ability, convergence speed and generalization ability of the neural network model, the RBF neural network is used to establish the model of braking deceleration prediction. To solve the problem that inefficient neurons occupy the network resources and affect the computing time, especially for the large sample size. The methods of removing

inefficient neurons in each training process and simplifying the radial basis function network structure under the condition of large data capacity through GGAP-RBF neural network [2] are used in this paper.

**3.3.1. RBF neural network**

RBF neural network is a kind of local perceptron network, which is a two layer forward network with a single hidden layer, including input layer, hidden layer and output layer [2], and the topological structure can be seen in Fig. 8. The signal is transmitted to the hidden layer by the input layer node, the nonlinear mapping in this process. It has the advantages of strong global approximation ability, fast convergence, strong generalization ability and good classification ability [2]. The input and output of RBF neural network is described as  $(x_i, y_i)$ [2], where  $i = 1, 2, 3, \dots, n$ .  $x_i$  is input vector with M dimension and  $y_i$  is the output value. The group i can be described as,

$$\Gamma^i = \{(x_i, y_i) : x_i \in D \in R^M, y_i \in R\} \quad (10)$$

Where  $R^M$  and  $R$  are M and 1 dimensional Euclidean space, respectively; D is the subset of  $R^M$ . The output can be described as,

$$f(x) = \sum_1^k \omega_k R_k(x) \quad (11)$$

Where, k is the number of neurons. In this paper, the Gauss function is chosen as the activation function, therefore, the hidden layer neuron function is given by,

$$R_k(x_i) = Radbas(\|w_k - x_i\| / \sigma_k) = e^{-\|w_k - x_i\|^2 / \sigma_k^2} \quad (12)$$

Where  $w_k$  is the radial basis of neuron k;  $\sigma_k$  is radial basis function width of neuron k. According to previous analysis of deceleration process, input vector of RBF can be described as,  $x_i = (u_a, \Delta u_a, i)^T$ . The output of the neural network is obtained as,

$$a(x_i) = \omega_0 + \sum_1^k \omega_k e^{-\|w_k - x_i\|^2 / \sigma_k^2} \quad (13)$$

Where, the deviation  $\omega_0 = 0.3$ ;  $\omega_k$  is the weight of neuron k;  $a(x_i)$  is the deceleration predicted.

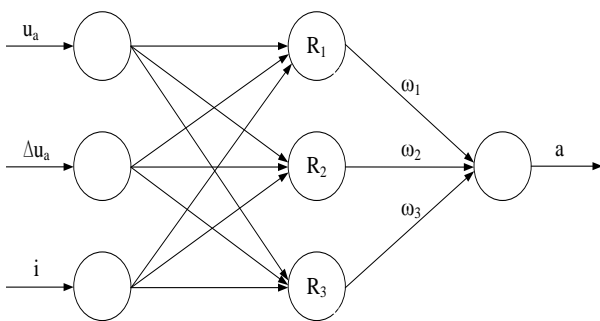


Fig. 8: Topological structure of RBF neural network

**3.3.2. Growth and pruning strategies**

The number of hidden layer neurons is usually equal to the number of samples in traditional neural network. The complexity of the network increases with the increase of the training samples, leading to the deterioration of network performance and seriously affects the computing performance. In this paper, the resource

growth strategy is used to determine whether we need to add new neurons to adapt to new training samples. After adding new hidden layer neurons, the decision method of network resource allocation is given by,

$$\begin{cases} \|x_i - w_{ir}\| > \varepsilon_i \\ e_i = y_i - f(x_i) > e_{\min} \end{cases} \quad (14)$$

Where  $e_i = y_i - f^{(i-1)}$  is the priori estimated error of the RBF network;  $w_{iy}$  is the central parameter of a neuron that has the shortest norm distance with neuron i;  $\varepsilon_i$  and  $e_{\min}$  are thresholds.  $\varepsilon_i$  is the distance threshold between new hidden layer neuron and current hidden layer neuron.  $e_{\min}$  is accuracy threshold of output value. In order to control the network scale and improve the network performance, the most effective way is to remove the neurons that have overlapping functions and have limited contribution to the prediction accuracy [3]. Therefore, pruning strategy is used to delete the inefficient neurons, which can improve the computing efficiency by simplifying the network structure [4]. The overall contribution rate of the network is the criterion to decide whether neuron k is inefficient using,

$$E_{sig}(k) < e_{\min} \quad (15)$$

**3.4. Training of GGAP-RBF neural network**

In order to train the GGAP-RBF neural network, road tests on different slopes were conducted. RLVB2SX VGPS speed sensor and SCA61T angle sensor were used in the tests. Since the braking habits of different drivers vary widely, 20 drivers were selected to participate in 3000 tests with different speeds and slopes. Those tests provide sufficient samples for training GGAP-RBF neural network model. Xi'an-Hanzhong section K76-K118 of Beijing-Kunming Expressway is chosen as test section, which can meet the demand of road slope and driving speed. The slopes of test section are 2.14%, 2.54% and 4.60%. The speed ranges are 20 - 40 km/h, 40 - 60km/h, 60 - 80km/h. The experimental data are used as the training samples of neural network and the required deceleration can be predicted. Test results under different operating conditions can be seen in Figs. 9 - 11. In Fig. 9, the deceleration range is from 0.01 m/s<sup>2</sup> to 0.45 m/s<sup>2</sup>. The deceleration is relatively larger at the beginning and gradually decreased. In Fig. 10, the range is from 0.03 m/s<sup>2</sup> to 0.28 m/s<sup>2</sup>. The deceleration range in Fig. 11 is from 0.10 m/s<sup>2</sup> to 0.42 m/s<sup>2</sup>. In summary, training sample of the deceleration of a heavy duty truck decreases with the increase of slope. The deceleration decreases with the decrease of speed.

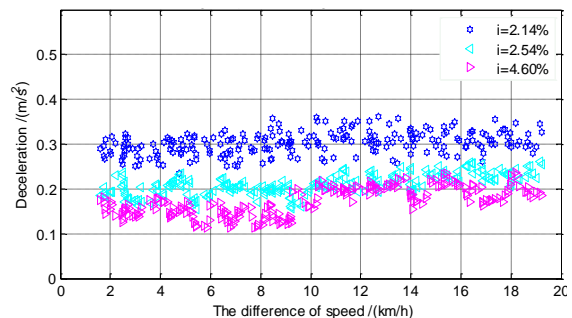


Fig. 9: Training sample in the range of 80km/h to 60km/h

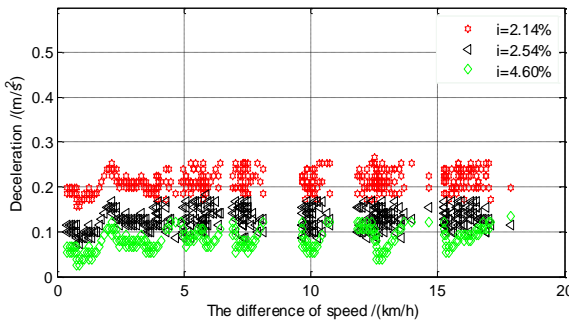


Fig. 10: Training sample in the range of 60km/h to 40km/h

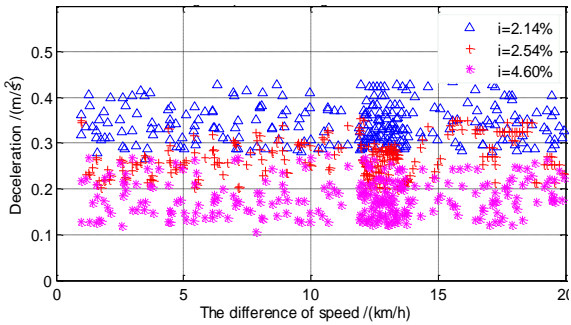


Fig. 11: Training sample in the range of 40km/h to 20km/h.

### 4. Simulation and verification

In order to realize the control strategy, establish a simulation model based on Matlab/Simulink is established and the accuracy of the model is verified by road tests. The simulation model, as shown in Fig. 12, includes vehicle module and prediction module of demand deceleration based on GGAP-RBF neural network, classification control module of endurance braking systems and velocity classification module. Road tests were conducted to verify the classification control strategy of endurance braking systems. In the tests, experienced driver were driving on the test section, the slope is 4.20% by setting the initial speed and the

target speed as 78km/h and 60km/h, respectively. The test and simulation results are shown in Figs. 13 and 14. As shown in Fig. 13, comparing the curve of the velocity variation, the simulation's velocity varies in synchronisation with the test results within 2km/h threshold in decelerating and stable stage. During the process, endurance brake classification is changed 3 times in the road test and it is shifted 2 times in the simulation model. The control strategy in this paper can effectively control the truck's velocity and reduce the driving fatigue under the premise of driving safety in the same situation.

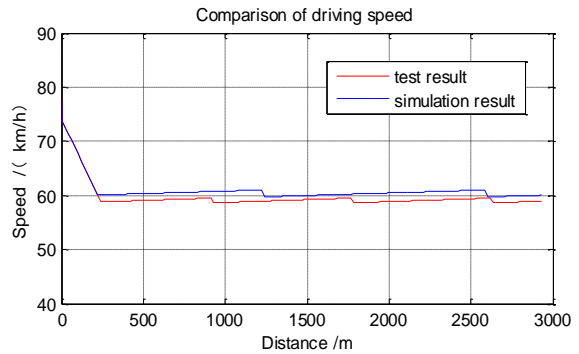


Fig. 13: Comparison of driving speed

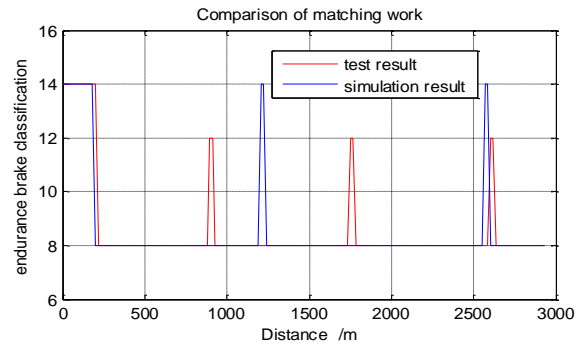


Fig. 14: Comparison of matching work

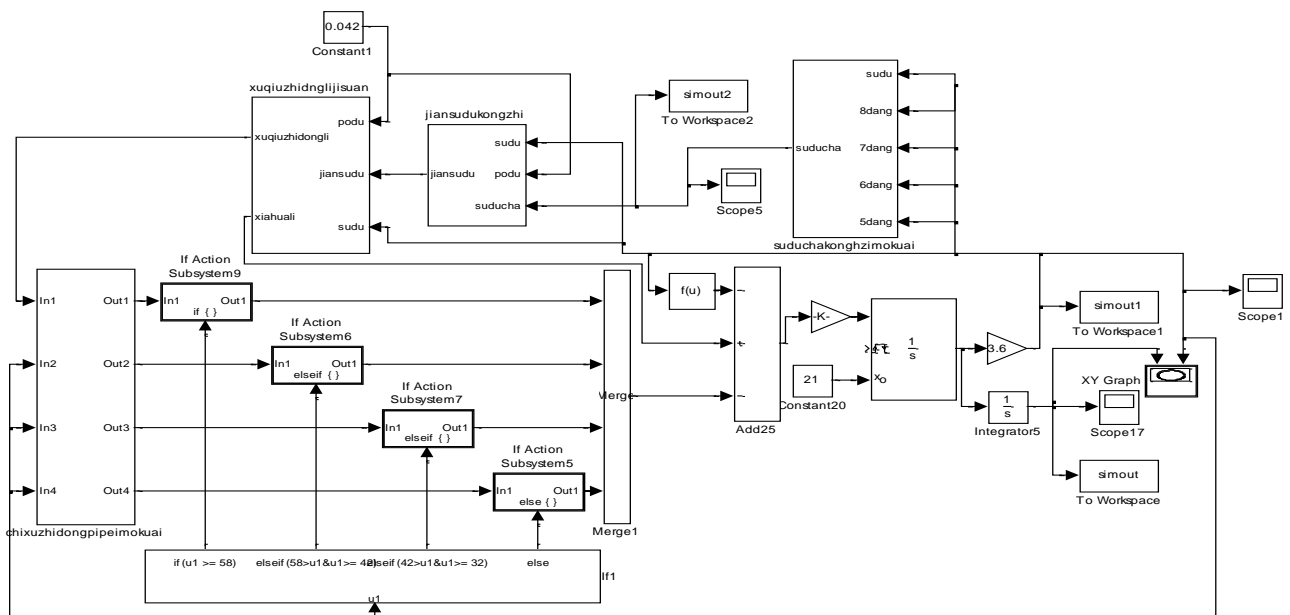
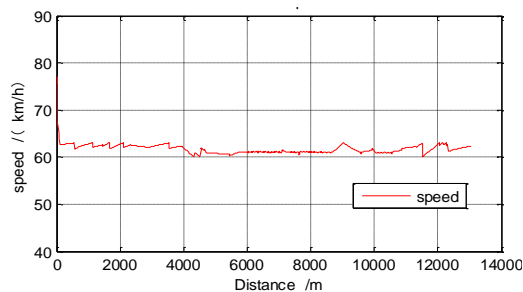


Fig. 12: Simulation model of classification control strategy

The road slopes varies randomly while heavy duty truck is driving on downhill. Thus, for further studying the applicability of the control strategy proposed, simulation research under variable slope conditions was conducted based on the road parameters of Xi'an-Hanzhong Expressway (from K44 + 140 to K56 + 550) as given in Table 3. In Fig. 15, first 100 meters, the truck is decelerating smoothly from 78km/h to 60km/h; subsequently, the velocity fluctuates within the range of 60km/h - 62km/h within the 2km/h threshold in stable state. The simulation has achieved an ideal control result. The endurance brake classifications as seen from Fig. 16 are matching accurately. The initial speed and expected speed were set to 78km/h and 60km/h; the distance is set to 13.16km. The simulation result shows that the control strategy proposed in this paper realized the endurance brake classification control, and it can adapt to the conditions that road slopes varies randomly.

**Table 3: Road parameters of Xi'an-Hanzhong Expressway**

| #  | Pile No. | Slope (%) | Len. (m) | #  | Pile No. | Slope (%) | Len. (m) |
|----|----------|-----------|----------|----|----------|-----------|----------|
| 1  | K44+144  | 2.80      | 780      | 11 | K52+200  | 2.60      | 300      |
| 2  | K44+920  | 3.70      | 830      | 12 | K52+500  | 4.50      | 790      |
| 3  | K45+750  | 2.90      | 950      | 13 | K53+290  | 3.00      | 410      |
| 4  | K46+700  | 1.65      | 600      | 14 | K53+700  | 4.50      | 650      |
| 5  | K47+300  | 2.13      | 1000     | 15 | K54+350  | 2.80      | 350      |
| 6  | K48+300  | 2.50      | 750      | 16 | K54+700  | 4.30      | 650      |
| 7  | K49+080  | 4.20      | 820      | 17 | K55+350  | 2.80      | 350      |
| 8  | K49+900  | 2.00      | 600      | 18 | K55+700  | 4.70      | 500      |
| 9  | K50+500  | 2.58      | 1120     | 19 | K56+200  | 3.00      | 350      |
| 10 | K51+620  | 4.50      | 580      | 20 | K56+550  | 5.00      | 750      |



**Fig. 15: The curve of the velocity variation**

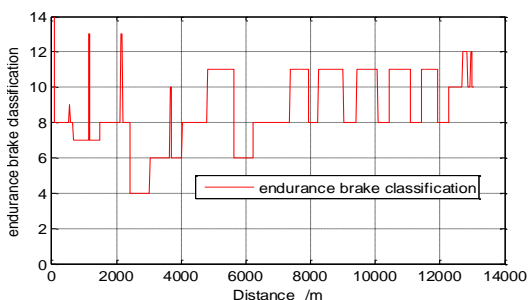


**Fig. 16: Changing of the endurance brake classification**

### 5. Conclusion

The classification control strategy of endurance braking systems based on the GGAP-RBF neural network proposed in this paper is an effective method to realize matching control for endurance braking systems. It can ensure that the truck decelerates smoothly and keeps it

running stably. It is of great significance to improve vehicle safety for truck on long downgrade roads.

### ACKNOWLEDGEMENTS:

This research was financially supported by Natural Science Foundation of China (Grant No. 51507013), the Natural Science Foundation of Shaanxi Province (Grant No. 2016JQ5012), Science and Tech. Research Project of Shaanxi Province (Grant No. 2016GY-043) and Chang'an University (Grant No. 310822151025 & 310822162019).

### REFERENCES:

- [1] J. Ma, Y. Chen, Q. Yu and R. Guo. 2003. Distance control for automotive's stopping with retarder, *China J. Highway and Transport*, 16(1), 108-112.
- [2] Y. Zhao, R. He and Y. Wang. 2008. Fuzzy distribution of braking forces in united braking system of downhill automobile at constant speed, *China Mech. Engg.*, 19(08), 1003-1007.
- [3] W. Dong, X. Yu and Y. Zhang. 2006. CVT control strategies for engine brake on long downhill of vehicle, *J. Jilin University*, 36(5), 650-653.
- [4] Y. Wu, G. Li and S. Lai. 2010. Simulation and analysis of the influence on the braking performance of the city bus with the use of eddy current brake, *J. Wuhan University of Tech.*, 32(12), 121-125.
- [5] Q. Yu, Y. Chen, J. Ma, R. Guo and Q. Zhang. 2004. A research on fuzzy control system with combination of engine brake, exhaust brake and retarder, *Automotive Engg.*, 26(4), 476-480.
- [6] P. Shi, Q. Yu, M. Yu and X. Zhao. 2016. Research on the brake temperature model of heavy duty truck on long downhill, *J. Highway and Transportation Research and Development*, 33(01), 147-152.
- [7] M. Mitschke and H. Wallentowitz. 2009. *Dynamik der Kraftfahrzeuge*, Tsinghua University Press, Beijing.
- [8] P. Shi, C. Yan and P. Zhang. 2016. Research on the long and steep downhill braking ability of heavy duty truck based on road experiment, *J. Southwest University*, (Natural Science Edition), 38(05), 194-200.
- [9] X. Zhao, L. Kang, G. Wang and J. Ma. 2014. SOC estimation based on BP neural network and characteristics of lead-acid battery, *Chinese J. Power Sources*, 38(5), 874-877.
- [10] Z. Pang. 2013. *System Identification and Adaptive Control of MATLAB Simulation*, Beihang University Press, Beijing.
- [11] J. Liu. 2003. *Radial Basis Function (RBF) Neural Network Control for Mechanical Systems*, Tsinghua University Press, Beijing.
- [12] R. Liu. 2015. *Study of Battery for Pure Electric Bus Based on GGAP-RBF Neural Network*, Chang'an University.
- [13] Y. Lu, N. Sundararajan and P. Saratchandran. 1998. Performance evaluation of a sequential minimal radial basis function (RBF) neural network learning algorithm, *J. IEEE Trans. Neural Network*, 9(2), 308-318. <https://doi.org/10.1109/72.661125>.
- [14] G. Huang, P. Saratchandran and N. Sundararajan. 2004. An efficient sequential learning algorithm for growing and pruning RBF networks, *J. IEEE Trans. System*, 34(6), 2284-2292. <https://doi.org/10.1109/TSMCB.2004.834428>.